Wetting and bonding characteristics of selected liquid-metals with a high power diode laser treated alumina bioceramic

J. Lawrence

Manufacturing Engineering Division, School of Mechanical & Production Engineering, Nanyang Technological University (NTU), Nanyang Avenue, Singapore 639798.

Correspondence

Dr. Jonathan Lawrence,

Manufacturing Engineering Division,

School of Mechanical & Production Engineering,

Nanyang Technological University (NTU),

Nanyang Avenue,

Singapore 639798.

Tel : (65) 6790 5542

Fax : (65) 6791 1859

e-mail: mjlawrence@ntu.edu.sg

Abstract

Changes in the wettability characteristics of an alumina bioceramic occasioned by high power diode laser (HPDL) surface treatment were apparent from the observed reduction in the contact angle. Such changes were due to the HPDL bringing about reductions the surface roughness, increases in the surface O_2 content and increases in the polar component of the surface energy. Additionally, HPDL treatment of the alumina bioceramic surface was found to effect an improvement in the bonding characteristics by increasing the work of adhesion. An electronic approach was used to elucidate the bonding characteristics of the alumina bioceramic before and after HPDL treatment. It is postulated that HPDL induced changes to the alumina bioceramic produced a surface with a reduced bandgap energy which consequently increased the work of adhesion by increasing the electron transfer at the metal/oxide interface and thus the metal-oxide interactions. Furthermore, it is suggested that the increase in the work of adhesion of the alumina bioceramic after HPDL treatment was due to a correlation existing between the wettability and ionicity of the alumina bioceramic; for it is believed that the HPDL treated surface is less ionic in nature than the untreated surface and therefore exhibits better wettability characteristics.

Keywords: High power diode laser (HPDL); Alumina; Bioceramic; Wettability; Bonding

1. Introduction

For many different types of materials, excimer laser radiation has been shown to be a viable means for transforming the surface properties of materials so as to bring about improvements to their wettability characteristics. Such materials include aluminium (Zhou & DeHosson 1993; 1994) and other metals (Heitz *et al.* 1992; Henari & Blau 1995; Olfert *et al.* 1996) coated with various ceramics, polymer materials like polyethylene terephthalate (PET) (Andrew *et al.* 1983; Watanabe *et al.* 1993), polyparaphenylene terephthalamide (PPTA) (Watanabe & Takata 1994) and polyether-etherketon (PEEK) (Laurens *et al.* 1998; 2000) and even textile fibres (Bahners 1993; Bahners *et al.* 1993). Comprehensive and detailed investigations by Song & Netravali (1998; 1998[1]; 1999) into the effects of excimer laser radiation on the interfacial characteristics of UHSPE fibres and epoxy resin revealed a considerable increase in the interfacial shear strength resulted after laser treatment. The considerable amount work conducted by Lawrence and Li is meaningful insofar as it demonstrates the practicability of employing different types of lasers to effect changes in the wettability characteristics of ceramics (1998; 1999; 1999[1]) metals (1999[2]; 2000) and polymers (2001) for improved adhesion and bonding. Moreover, Lawrence recently identified the reasons for the changes in the wetting characteristics after laser surface treatment with regard to changes in the material's surface topography, surface composition and surface energy for ceramics (2002) and metals (2002[1]).

This paper examines the interfacial bonding and adhesion characteristics of a number of liquid-metals on the untreated and high power diode laser (HPDL) treated surface of a alumina bioceramic in electronic terms. Furthermore, this investigation will provide valuable insight and permit a fuller understanding of the adhesion and bonding mechanisms active in the alumina bioceramic, especially the alterations to these mechanisms after HPDL treatment.

Some time ago McDonald & Eberhart (1965) proposed that there were two different surface sites for bonding metal atoms of liquid transition metals with Al_2O_3. The first type took the form of van der Waals interactions between the metal atoms and the O^{2-} anions present on the Al_2O_3 surface. The second type involves the metal/O_2 chemical bonds whose energy was assumed to be proportional to the free energy of the metal oxide formation. Consequently the work of adhesion can be expressed as the sum of these two bonding energies. Work by Chatain *et al.* (1986) elaborated further and found that it was necessary to take into account the metal/Al chemical interactions along with the metal/O_2 reactions. Indeed, this approach yielded good agreement with an empirical equation comprising bulk

thermodynamic quantities of both metal/O_2 and metal/Al_2O_3 bonds. Although these approaches are undoubtedly useful, Stoneham & Tasker (1985) maintain that many phenomena associated with metal/non-metal interfaces with large dielectric constant mismatch can be explained in terms of the image interactions. More particularly, it was stated that the chief contributor to adhesion between non-reactive metals and oxides is the electrostatic interaction between ionic charges in the oxide and the induced image charges in the metal. This notion was substantiated theoretically by Johnson & Pepper (1982) who showed that, for transition metals in contact with sapphire, the primary interaction occurred between the metal atoms and the O^{2-} anions present on the sapphire surface and was essentially covalent. Further, Hicter *et al.* (1988) suggested that the adhesion between a non-reactive metal and Al_2O_3 was brought about through electron transfer from the metal into the Al_2O_3 conduction band which was assumed be initially empty. Using an electronic approach, an encompassing and comprehensive study by Li (1992) found that the work of adhesion of non-reactive liquid-metals with transition metal carbides was a simultaneous function of the valence electron concentrations of both metal and carbide. In the same way, the work of adhesion of different metals on TiC was found to increase linearly with increasing electron density at the boundary of the Wigner-Seitz cell of the corresponding metals. At the same time, the work of adhesion of Cu on a number of transition metal carbides was seen to increase with decreasing thermodynamic stability of the carbides. From this work it was concluded that the interactions between a metal and a carbide are basically metallic in nature, resulting from the overlapping of the valence electrons at the metal/carbide interface. What is more, Li (1992[1]) extended this approach to reveal that this dependency of the work of adhesion on the electron density of the liquid-metal and the thermodynamic stability of the solid compound was the case for various liquid-metal/solid-ionocovalent oxides.

2. Experimental procedures

2.1. Alumina bioceramic specifications

The alumina bioceramic studied in this work was alpha-alumina which is typically used for hip ball & cup replacements. For the purpose of experimental convenience the alpha-alumina was fabricated into blocks (25 x 25 x 5 mm^3) prior to laser treatment. The alpha-alumina used was 99.4% pure Al_2O_3 with impurities of CaO, Fe_2O_3, K_2O, MgO, Na_2O, SiO_2 and TiO_2 constituting the remaining 0.6%. In order to carry out analytical analyses of the untreated and HPDL treated specimens, they were

sectioned with a cutting machine (Struers, Ltd.) using a diamond rimmed cutting blade and examined using optical microscopy, scanning electron microscopy (SEM), energy disperse X-ray analysis (EDX) and X-ray diffraction (XRD) techniques.

2.2. High power diode laser processing procedures

The HPDL (Rofin-Sinar GmbH DL 020 S) used in this work emitted a high order mode beam at 808 ±10 nm and was operated in the CW mode with optical powers ranging from 40-120 W. A schematic illustration of the laser processing experimental arrangement is given in Figure 1. The HPDL beam was delivered to the work area by means of an optical fibre 10 m long and of 1500 μm core diameter. The end of the fibre was connected to a focusing lens assembly with a focal length of 42 mm and was mounted on the z-axis of a 3-axis CNC gantry table. This arrangement produced a defocused HPDL beam with a spot diameter of 2.5 mm. The alumina bioceramic was irradiated with the HPDL beam by traversing the samples beneath the beam using the x- and y-axis of the CNC gantry table at a speed of 360 - 480 mm/min with an O_2 process gas being coaxially blown at a rate of 3 l/min.

2.3. Wettability and bonding characteristics analysis procedures

To examine the wetting and surface energy characteristics of the alumina bioceramic, and hence quantify any surface energy changes in the material resulting from HPDL interaction, a series of control experiments were carried out using the sessile drop technique with a variety of liquids with known surface energy properties. The control test liquids were: human blood; human blood plasma; glycerol and 4-octanol. This particular test liquid series was selected as it has been shown in previous studies (Agathopoulos & Nikolopoulos 1995; Lawrence & Li 1999; 2001) to be most suitable for ceramic materials. The experiments were conducted in normal atmospheric conditions at a temperature of 20^0C $\pm 2^0$C with the temperature of the liquids themselves throughout the experiments also being maintained at around 20^0C. The droplets were released onto the surface of the test alumina bioceramic (HPDL treated and untreated) from the tip of a micropipette, with the resultant volume of the drops being approximately 6 x 10^{-3} cm^3. Each experiment lasted for three minutes with profile photographs of the sessile drops being obtained every minute and the contact angle, θ, subsequently being measured. The standard deviation due to experimental error was calculated as being $\pm 0.2^0$.

To obtain a fuller appreciation of the adhesion and bonding mechanisms active in the alumina bioceramic, before and after HPDL treatment, wettability experiments were conducted using selected

liquid-metals. In this way it was possible to examine the adhesion and bonding characteristics from an electronic stand point. The metals chosen were: Al; Cu; Fe; Mn; Pb and Sn and were supplied in cubes of 3 x 3 x 3 mm^3. The metals were selected on account of the fact that full details of their surface energy characteristics. The experiments were completed by placing a cube of each metal on the untreated and HPDL treated surface of the alumina bioceramic samples. The samples were then placed in turn inside a vacuum furnace whereupon each sample was heated to the various melting temperatures of the metals at a rate of 75^0C/min in a vacuum of 2 x 10^{-5} torr. At the appropriate time the liquid-metal sessile drops were photographed through the glass window of the furnace every minute for three minutes. The sessile drop photographs were subsequently analysed to obtain a value for θ. The standard deviation due to experimental error was calculated as being $\pm 0.4^0$.

3. Wetting and the work of adhesion at the liquid-metal/ceramic interface

In practice, for wetting to occur, θ, must be less than 90^0, otherwise if θ is greater than 90^0 then the liquid does not wet the solid and no adhesion occurs (Fowkes 1964). When a drop of liquid is brought into contact with a flat solid surface, the final shape taken by the drop, and thus whether it will wet the surface or not, depends upon the relative magnitudes of the molecular forces that exist within the liquid (cohesive) and between the liquid and the solid (adhesive) (Fowkes 1964). The index of this effect is θ and it is related to the solid and liquid surface energies, γ_{sv} and γ_{lv}, and the solid-liquid interfacial energy γ_{sl}, through the principle of virtual work expressed by the rearranged Young's equation:

$$\cos\theta = \frac{\gamma_{sv} - \gamma_{sl}}{\gamma_{lv}} \qquad (1)$$

Clearly, to achieve wetting γ_{sv} should be large, while γ_{sl} and γ_{lv} should be small. Hence liquids of a lower surface tension will always spread over a solid surface of higher surface tension in order to reduce the total free-energy of the system (Zisman 1964). This is on account of the fact that the molecular adhesion between solid and liquid is greater than the cohesion between the molecules of the liquid (Fowkes 1964).

In fundamental terms, the driving force for the formation of a liquid-metal/ceramic interface is the energy relinquished when the intimate contact between the metal and the ceramic is formed. This

driving force is usually characterised by the adhesion energy. The adhesion energy, or work of adhesion, W_{ad}, is defined as the work per unit area which needs to be provided to separate reversibly a solid/liquid interface so as to create distinct solid/vapour and liquid/vapour interfaces. Thus

$$W_{ad} = \gamma_{sv} + \gamma_{lv} - \gamma_{sl} \tag{2}$$

If one takes into account Young's equation then Equation (1) can be rearranged to form the Young-Dupre equation. Thus the W_{ad} can be expressed as

$$W_{ad} = \gamma_{lv}(1 + \cos\theta) \tag{3}$$

In this way experimental values of W_{ad} can be determined from the γ_{lv} value of the liquid and the value of θ produced when the liquid is in contact with the solid.

Generally the value of W_{ad} in metal/ceramic systems can be expressed as the sum of the different contributions of the interfacial interactions between two phases:

$$W_{ad} = W_{equil} + W_{non-equil} \tag{4}$$

where $W_{non\text{-}equil}$ denotes the non-equilibrium contribution to the work of adhesion when a chemical reaction takes place at the metal/ceramic interface, while W_{equil} represents the equilibrium contribution which corresponds to non-reactive systems. This contribution can be further divided into two separate terms: $W_{chem\text{-}equil}$, which is the cohesive energy between the two contacting phases that results from the establishment of chemical equilibrium bonds achieved by the mutual saturation of the free valences of the contacting surfaces and W_{VDW}, which signifies the van der Waals interaction or dispersion forces. As such, Equation (4) becomes

$$W_{ad} = W_{chem-equil} + W_{VDW} + W_{non-equil} \tag{4a}$$

4. Analysis of the wetting and bonding characteristics

4.1. High power diode laser interaction with the alumina bioceramic and the effects thereof on wettability characteristics

In order to investigate accurately the bonding characteristics of the alumina bioceramic, both before and after HPDL surface treatment, it is essential that consideration is given to the wettability characteristics changes that are effected by HPDL interaction. Using a selected control test liquid

series it can be seen from Table 1 that interaction of the alumina bioceramic with the HPDL beam resulted in the θ between the alumina bioceramic and the control test liquids reducing appreciably, implying that marked changes in the wettability characteristics have been realised. Previous studies have shown that such laser-induced changes in the wettability characteristics of ceramics are due to changes in three factors: the surface roughness; the surface O_2 content and the surface energy (Lawrence 2002).

4.1.1. Surface roughness

Irregularities on the surface of a material that cause roughness generally take the form of grooves. Rough grooves on a surface can be categorised as either radial or circular grooves. In practical terms, any rough surface can be represented by a combination of these two cases (Zhou &DeHosson 1995), with two roughness parameters being defined as the Wenzel type, D_R (Wenzel 1936) and the Cassie/Baxter type, F_R (Cassie & Baxter 1944). In the case that wetting spreads radially, as is the likely case with the alumina bioceramic, then the resulting radial contact angle, θ_{rad}, is related to the theoretical contact angle, θ_{th}, by

$$\cos\theta_{rad} = D_R\left(1 - F_R\right)\cos\theta_{th} - F_R \tag{14}$$

According to Neumann (1974), only if F_R is equal to zero, then a model similar to that for heterogeneous solid surfaces can be developed in order to account for surface irregularities, being given by a rearrangement of Wenzel's equation:

$$\gamma_{sl} = \gamma_{sv} - \left(\frac{\gamma_{lv}\cos\theta_w}{r}\right) \tag{15}$$

where, r is the roughness factor defined as the ratio of the real and apparent surface areas and θ_w is the contact angle for the wetting of a rough surface. It is important to note that Wenzel's treatment is only effective at the position of wetting triple line (Zhou & DeHosson 1995). Nonetheless, it is evident from Equation (15) that if the roughness factor, r, is large, that is the solid surface is smooth, then γ_{sl} will become small, thus, a reduction in the contact angle will be inherently realised by the liquid if $\theta_w<90^0$. Conversely, if $\theta_w>90^0$ then the opposite will be observed. Although other, more sophisticated approaches may be taken to examine the effects of surface roughness on wetting (Palasantzas & DeHosson 2001), for this present study the use of Equation (15) is quite sufficient.

Reductions in the surface roughness of the alumina bioceramic were observed (using a Taylor-Hobson Surtronic 3+ profileometer) after interaction with the HPDL beam (see Table 1). Similar results were obtained by Nicolas *et al.* (1997), who observed that excimer laser treatment of a ZrO_2 ceramic resulted in a smoother surface and Feng *et al.* (1998), who noted that θ was inversely proportional to surface roughness.

4.1.2. Surface O_2 contact

The O_2 content of a material's surface is an influential factor governing the wetting performance of the material; where an increase will inherently produce a reduction in θ, and vice versa (Ueki *et al.* 1986; Li 1993). Now, wetting is governed by the first atomic layers of the surface of a material, so to determine the element content of O_2 at the surface of the alumina bioceramic, it was necessary to examine the surface using XPS. The results of the XPS analysis of the alumina bioceramic in terms of the surface O_2 content are given in Table 1.

4.1.3. Surface energy

Surface energy, γ, arises from a variety of intermolecular forces whose contribution to the total surface energy is additive (Fowkes 1964). The majority of these forces are functions of the particular chemical nature of a certain material, and as such the total surface energy comprises of γ^p (polar or non-dispersive interaction) and γ^d (dispersive component; since van der Waals forces are present in all systems regardless of their chemical nature). Therefore, the surface energy of any system can be described by (Fowkes 1964)

$$\gamma = \gamma^d + \gamma^p \tag{16}$$

Likewise, W_{ad} can be expressed as the sum of the different intermolecular forces that act at the interface (Fowkes 1964):

$$W_{ad} = W_{ad}^d + W_{ad}^p = 2\left(\gamma_{sv}^d \gamma_{lv}^d\right)^{1/2} + 2\left(\gamma_{sv}^p \gamma_{lv}^p\right)^{1/2} \tag{17}$$

By equating Equation (17) with Equation (2), θ for solid/liquid systems can be related to the surface energies of the respective liquid and solid by

$$\cos\theta = \frac{2\left(\gamma_{sv}^d \gamma_{lv}^d\right)^{1/2} + 2\left(\gamma_{sv}^p \gamma_{lv}^p\right)^{1/2}}{\gamma_{lv}} - 1 \tag{18}$$

Fowkes (1964) has stated that γ_{sv}^{d} can be estimated by using Equation (18) and plotting the graph of cos θ against $(\gamma_{lv}^{d})^{1/2}/\gamma_{lv}$ (see Figure 2). Hence the value of γ_{sv}^{d} is estimated by the gradient $(=2(\gamma_{sv}^{d})^{1/2})$ of the line which connects the origin (cos θ = -1) with the intercept point of the straight line (cos θ against $(\gamma_{lv}^{d})^{1/2}/\gamma_{lv}$) correlating the data point with the abscissa at cos θ = 1.

It is not possible to determine the value of the polar component of the alumina bioceramic surface energy directly from Figure 2 since the intercept of the straight line (cos θ against $(\gamma_{lv}^{d})^{1/2}/\gamma_{lv}$) being at $2\left(\gamma_{sv}^{p}\gamma_{lv}^{p}\right)^{1/2}/\gamma_{lv}$ and as such, only referring to individual control liquids and not the control liquid system as a whole. Having said that, it has been established that the entire amount of the surface energies owing to dispersion forces of either the solids or the liquids are active in the wettability performance (Fowkes 1964; Good & Girifalco 1960). Therefore it is possible to calculate the dispersive component of the work of adhesion from Equation (17). The results reveal that for each particular control liquid in contact with both the untreated and HPDL treated alumina bioceramic surfaces, W_{ad} can be correlated with W_{ad}^{d} by the relationship

$$W_{ad} = aW_{ad}^{d} + b \tag{19}$$

Also, for the control test liquids used, a linear relationship between the dispersive and polar components of the control test liquids surface energies has been deduced which satisfies the equation

$$\left(\gamma_{lv}^{p}\right)^{1/2} = 0.45\left(\gamma_{lv}^{d}\right)^{1/2} + 1.15 \tag{20}$$

By introducing Equation (19) into Equation (17) and rearranging, then

$$W_{ad}^{p} = (a-1)W_{ad}^{d} + b \tag{21}$$

or

$$\left(\gamma_{sv}^{p}\right)^{1/2}\left(\gamma_{lv}^{p}\right)^{1/2} = (a-1)\left(\gamma_{sv}^{d}\right)^{1/2}\left(\gamma_{lv}^{d}\right)^{1/2} + \frac{b}{2} \tag{22}$$

What is more, by introducing Equation (20) into Equation (22) and differentiating with respect to $\left(\gamma_{lv}^{d}\right)^{1/2}$, considering that $\left(\gamma_{sv}^{d}\right)^{1/2}$ and $\left(\gamma_{sv}^{p}\right)^{1/2}$ are constant, then the following is valid:

$$\left(\gamma_{sv}^{p}\right)^{1/2} = \frac{\left(\gamma_{sv}^{d}\right)^{1/2}(a-1)}{0.45} \tag{23}$$

Now, the value of *a* for the untreated and HPDL treated alumina bioceramic can be determined from a plot of Equation (19) (0.74 and 1.26 respectively) and γ_{sv}^{d} has already been determined for the untreated and HPDL treated alumina bioceramic from Figure 2. As such it is possible to calculate γ_{sv}^{p} for untreated and HPDL treated alumina bioceramic by simply using Equation (23).

It is evident from Table 1 that the HPDL melting of the surface of the alumina bioceramic leads to a reduction in the total surface energy whilst increasing γ_{sv}^{p}, thereby improving the action of wetting and adhesion. Such changes in the surface energy of the alumina bioceramic after HPDL melting are due to the fact partial vitrification of the surface is occasioned, a transition that is known to bring about an increase in γ_{sv}^{p} (Lawrence *et al.* 1998).

It is important to realise at this point that owing to the long range ionic interactions in the alumina bioceramic and the composite nature of the interfaces between the alumina bioceramic and the control test liquids, it is probable that the thermodynamically defined total solid surface energy, as defined in Equation (16), will be higher than the sum of the γ^{d} and γ^{p} components of the surface energy. Indeed, the derivations that lead to Equation (18) can only be done under the specific assumption that the ionisation potentials are all equal and that dipole-dipole random orientation interactions dominate over dipole-induced dipole random interactions. Still, the increase in (excess) surface free energy will doubtless be less then the increase in the total lattice energy. On the other hand, an absorbed liquid layer may shield the ionic fields substantially. Consequently, all the data derived from Equations (16) - (23) should be considered as being semi-empirical. Nevertheless, as the studies by Agathopoulos & Nikolopoulos (1995) and Lawrence (1999; 2001; 2002) found, it is reasonable to conclude from the data obtained from Equations (16) - (23) that HPDL treatment of the alumina bioceramic has caused an increase γ^{p} .

4.2. The bonding characteristics between the high power diode laser treated alumina bioceramic and the selected liquid-metals

When two dissimilar materials are brought into contact, complex combinations of a range of bonding mechanisms actually occur, varying according to the types of materials used (Greenhut 1991). For

most materials in intimate contact with the alumina bioceramic, the mechanisms active will principally involve physical bonding (van der Waals forces), chemical bonding and electronic reactions (Greenhut 1991). In the particular case of the alumina bioceramic, the primary bonding mechanism active will be physical. This is because adhesion between many materials is assured by electron transfer and is therefore related to bandgap energy (Li 1995). Thus, for non-conducting materials with large bandgaps such as the alumina bioceramic, there will be very few free charges inside the ceramic crystals, even at elevated temperatures. In this case the electron transfer at the interface will be minimal as the electron transfer depends exclusively on the concentration of free charges in the ceramic crystal (Li 1995). As a result, W_{VDW} will be the major contributor to W_{ad} in Equation (4(a)). Even so, evidence of the action of bonding mechanisms other than van der Waals forces has been observed in previous studies.

A direct indication of the energetical interactions that take place between the solid and liquid phases of such materials when in contact can be gleaned from W_{ad}; with increases denoting stronger interactions. As Table 2 shows, from measurements of θ for selected liquid-metals in contact with the surface of the alumina bioceramic, it was possible to calculate the corresponding value of W_{ad} using Equation (3). These W_{ad} values are plotted as a function of the electron density, $n_{w\text{-}s}$, at the boundary of the Wigner-Seitz cell of the corresponding metals in Figure 3. As can be seen from Figure 3, a general increase in W_{ad} between the alumina bioceramic and the selected liquid-metals has been occasioned after HPDL treatment. Since metal-oxide interactions are assured by electron transfer at the metal/oxide interface, then it would appear from Figure 3 that such an increase has resulted from HPDL interaction. The intensity of the electron transfer at the interface depends on the electron density of the metal on the one hand, and on the concentration of the holes in the valence band of the oxide on the other. So if the oxide type is set and the liquid-metals in contact with it are changed, then the intensity of the electron transfer at the interface would exclusively be a function of the electron density of the liquid-metals and would increase accordingly with the electron density of the metals. This occurrence is borne out somewhat by the linear relationship seen between W_{ad} for the selected liquid-metals with the alumina bioceramic (untreated and HPDL treated) on the electron density at the boundary of the Wigner-Seitz cell of the corresponding metals. Similarly, if one considers Equation (24), which shows the relationship between the concentration of holes in the valence band (which is equal to the number of electrons in the conduction band) for an ideal pure oxide crystal, C, and the bandgap energy, E_g

$$C = C_o \exp\left(\frac{-E_g}{2KT}\right) \tag{24}$$

where and C_o is a constant, K is Boltzmann's constant and T is temperature, then it can be seen that the concentration of holes in the valence band increases with a decrease in the bandgap energy. Accordingly, the intensity of electron transfer at the liquid-metal/oxide interface increases with decreasing bandgap energy of the oxide. Thus it is possible to say that W_{ad} of any given liquid-metal on an oxide will increase, with θ decreasing accordingly due to Equation (3), with a decrease in the bandgap energy of the oxide. This being the case, it is reasonable to maintain that Figure 3 implies that HPDL interaction with the alumina bioceramic has brought into being a surface with a reduced bandgap energy since W_{ad} has evidently increased after HPDL treatment, whilst at the same time a reduction in θ has been realised (see Table 2).

Findings by Vijh (1970) revealed a linear correlation between the bandgap energy of a number of different oxides and the ratio r_i/r_m of the ionic radius, r_i, to the metallic radius, r_m, of certain oxide metals. Based on the above discussions it is likely that a correlation between the wetting properties of the oxide metals and the ratio r_i/r_m exists. Indeed, the ionicity of a binary solid has been defined in terms of the electronegativity of the two components making up the solid, with the values of these electronegativities being derived from the excess bond energy above the purely covalent component (Vijh 1970; Li 1992[1]). Clearly, if there is a correlation between bandgaps and bond energies, and if the electronegativities are derived from bond energies, then it follows that there is a correlation between bandgaps and electronegativities. With this rationale a correlation between wettability and ionicity is quite conceivable. Thus it can be assumed that as the ionicity of a ceramic increases, the material's propensity to wet will decease and vice versa. The observed increase in W_{ad} in Figure 3 and the corresponding decrease in θ recorded in Table 2 after HPDL of the alumina bioceramic appear to support this assumption. It is, therefore, highly probable that the surface of the alumina bioceramic produced by HPDL interaction will be less ionic in nature than the untreated surface and will in turn have increased wettability characteristics.

5. Conclusions

High power diode laser (HPDL)-induced changes in the wettability characteristics of an alumina bioceramic are effected as a result of: (i) an ideal level of melting and resolidification being induced

which in turn causes a reduction in the surface roughness, thereby directly reducing the contact angle, θ, (ii) an increase in the surface O_2 content of the alumina bioceramic after HPDL treatment which intrinsically brings about a decrease in θ and (iii) the increase in the polar component of the surface energy, γ_{sv}^{p}, of the alumina bioceramic resulting from the HPDL induced surface melting and resolidification which consequently creates a more polar partially vitrified microstructure.

From an electronic perspective, the bonding characteristics of the alumina bioceramic before and after HPDL treatment were determined from wettability experiments carried out with selected liquid-metals. It was found that HPDL surface treatment yielded an overall increase in the work of adhesion, W_{ad}, and a corresponding reduction in θ, between the alumina bioceramic and the selected liquid-metals. It is believed that this observed increase in W_{ad} and the matching reduction in θ resulted from the HPDL induced changes to the alumina bioceramic creating a surface with a reduced bandgap energy, which is significant, for metal-oxide interactions are assured by electron transfer at the metal/oxide interface. In addition, correlations between bandgaps and bond energies, and in turn bandgaps and electronegativities mean that a correlation between the wettability and ionicity of the alumina bioceramic is certainly possible, with increases in the ionicity of the alumina bioceramic leading to a decreased disposition to wet. Based on this notion it is asserted that the observed increase in W_{ad} and the corresponding decrease in θ of the alumina bioceramic after HPDL is due to the surface being less ionic in nature than the untreated surface, thereby inherently increasing the wettability characteristics.

References

Agathopoulos, S. & Nikolopoulos, P. 1995 *J. of Biomed. Mater. Res.* **29**, 421-429.

Andrew, J.E. Dyer, P.E. Forster, D. & Key, P.H. 1983 *Appl. Phys. Lett.* **43**, 717-718.

Bahners, T. Kesting, W. & Schollmeyer, E. 1993 *Appl. Surf. Sci.* **69**, 12-15.

Bahners, T. 1993 *Opt. Quan. Elec.* **27**, 1337-1348.

Cassie, A.B.D. & Baxter, S. 1944 *Trans. Faraday Soc.* **40**, 546-552.

Chatain, D. Rivollet, I & Eusthapolous, N. 1986 *J. Chem. Phys.* **83**, 561-567.

Feng, A. McCoy, B.J. Munir, Z.A. & Cagliostro, D. 1998 *Mat. Sci. & Eng. A* **1**, 50-56.

Fowkes, F.M. 1964 *Ind. Eng. Chem.* **56**, 40-52.

Good, R.J. & Girifalco, L.A. 1960 *J. Phys. Chem.* 64, 561-565.

Greenhut, V.A. 1991 Surface Considerations for joining ceramics and glasses, In *Engineered Materials Handbook: Adhesives and Sealants*, (Ed. H.F. Brinson), pp 298-311. Metals Park: ASM International.

Heitz, J. Arenholz, E. Kefer, T. Bäuerle, D. Hibst, H. & Hagemeyer, A. 1992 *Appl. Phys. A* **55**, 391-392.

Henari, F. & Blau, W. 1995 *Appl. Optics* **34**, 581-584.

Hictor, P. Chatain, D. Pastural A. & Eusthapolous, N. 1988 *J. Chem. Phys.* **85**, 941-945.

Johnson, K.H. & Pepper, S.V. 1982 *J. Appl. Phys*. **53**, 6634-6637.

Laurens, P. Sadras, B. Decobert, F. Arefiknonsari, F. & Amouroux, J. 1998 *Int. J. Adhesion Adhesives* **18**, 19-27.

Laurens, P. Ould Bouali, B. Meducin, F. & Sadras, B. 2000 *Appl. Surf. Sci.* **154/155**, 658-663.

Lawrence, J. Li, L. & Spencer, J.T. 1998 *Optics Laser Tech.* **30**, 205-214.

Lawrence, J. & Li, L. 1999 *J. Phys. D* **32**, 1075-1082.

[1]Lawrence, J. & Li, L. 1999 *Appl. Surf. Sci.* **138/139**, 388-393.

[2]Lawrence, J. & Li, L. 1999 *J. Phys. D* **32**, 2311-2318.

Lawrence, J. & Li, L. 2000 *Appl. Surf. Sci.* **154/155**, 664-669.

Lawrence, J. & Li, L. 2001 *Mater. Sci. Eng. A.* **303**, 142-149.

Lawrence, J. 2002 *Proc. Royal Soc. A* **2026**, 2445-2463.

[1]Lawrence, J. 2002 *J. Laser Apps.* **14**, 107-113.

Li, J.G. 1992 *J. Mater. Sci. Lett.* **11**, 903-905.

[1]Li, J.G. 1992 J. Am. Ceram. Soc. 75, 3118-3126.

Li, J.G. 1993 *Rare Met.* **2**, 84-96.

Li, J.G. 1995 *Mater. Lett.* **22**, 169-174.

McDonald, J.E. & Eberhart, J.G. 1965 *Trans. Metall. Soc.* **233**, 512-517.

Neumann, A.,W. 1974 *Adv. Colloid Interface Sci.* **4**, 438.

Nicolas, G. Autric, M. Marine, W. & Shafeev, G.A. 1997 *Appl. Surf. Sci.* **109/110**, 289-292.

Olfert, M. Duley, W. & North, T. 1996 Surface treatment and film deposition. In *Laser Processing* (Eds. J. Mazumder, O. Conde, R. Villan and W. M. Steen), pp. 479-490. Amsterdam: Kluwer Academic Publishers.

Palasantzas, G. & DeHosson, J. Th. M. 2001 *Acta Mater.* **49**, 3533-3538.

Song, Q. & Netravali, A.N. 1998 *J. Adhesion Sci. Tech.* **9**, 957-982.

[1]Song, Q. & Netravali, A.N. 1998 *J. Adhesion Sci. Tech.* **9**, 983-998.

Song, Q. & Netravali, A.N. 1999 *J. Adhesion Sci. Tech.* **13**, 501-516.

Stoneham, A.M. & Tasker, P.W. 1985 *J. Phys. C* **18**, 543-548.

Ueki, M. Naka, M.& Okamoto, I. 1986 *J. Mater. Sci. Lett.* **5**, 1261-1262.

Vijh, A.K. 1970 *J. Mater. Sci.* **5**, 379-382.

Watanabe, H. Shimizu, H. & Takata, T. 1993 *Sen'-i Gakkaishi* **49**, 616-623.

Watanabe, H. & Takata, T. 1994 *J. Adhesion Sci. Tech.* **8**, 1425-1438.

Wenzel, R.N. 1936 *Ind. Eng. Chem.* **28**, 988- 994.

Zhou, X.B. & DeHosson, J.T.M. 1993 *J. de Phys. IV* **3**, 1007-1011.

Zhou, X.B. & DeHosson, J.T.M 1994 *Acta Metall. Mater.* **42**, 1155-1162.

Zhou, X.B. & DeHosson, J.T.M 1995 *J. Mat. Research* **10**, 1984-1992.

Zisman, W.A. 1964 Contact angle, wettability and adhesion. In: *Advances in Chemistry Series 43* (Ed. R.F. Gould), pp 1-51. Washington DC: American Chemical Society.

Figure 1

Schematic diagram of the experimental set-up for the HPDL treatment of the alumina bioceramic.

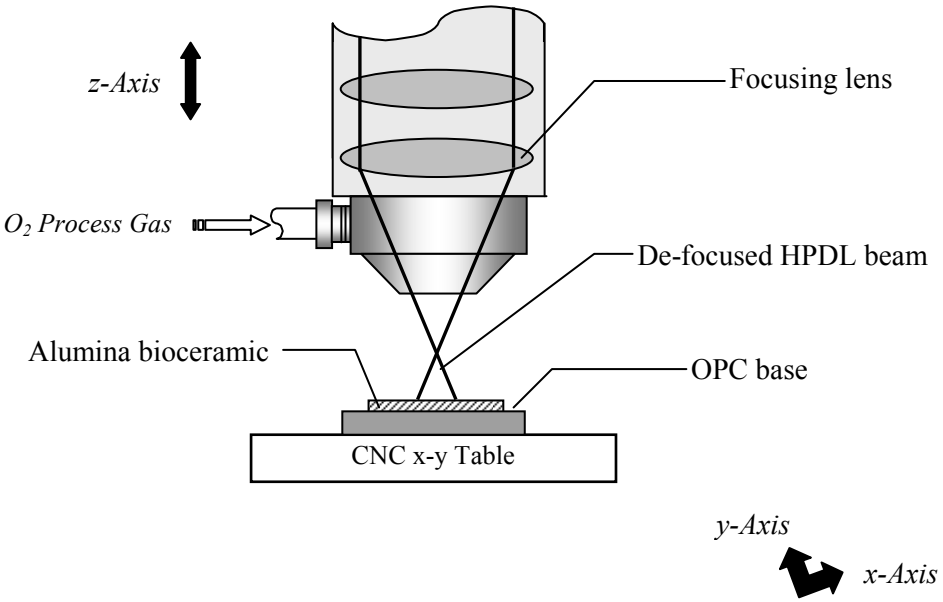

Figure 2

Plot of cos θ against $\left(\gamma_{lv}^{d}\right)^{1/2}/\gamma_{lv}$ for the alumina bioceramic in contact with the wetting test control liquids, before and after HPDL treatment.

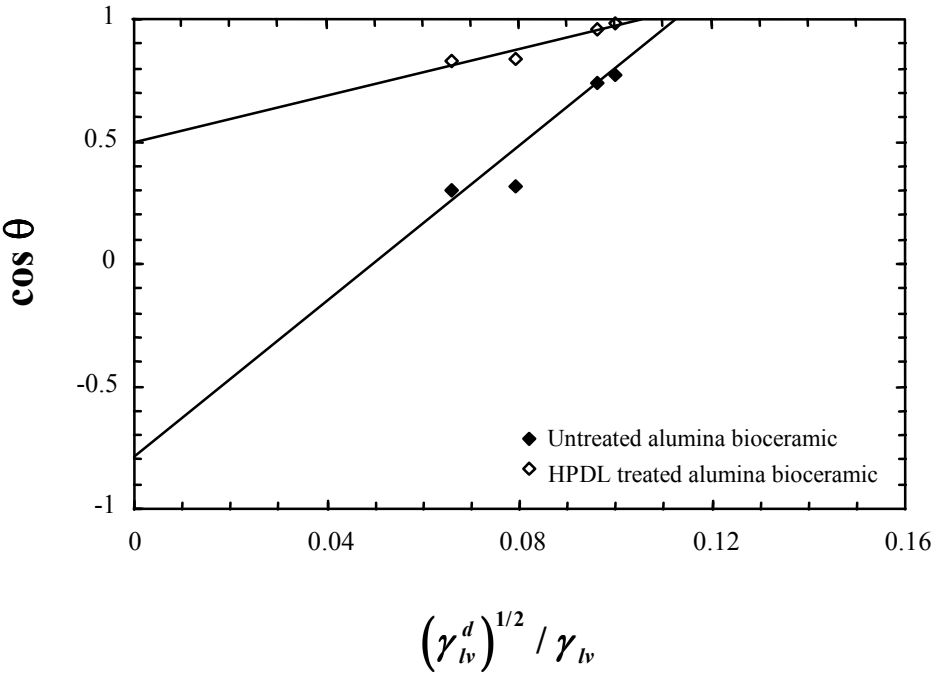

Figure 3

Work of adhesion of selected liquid-metals with the untreated and HPDL treated alumina bioceramic in terms of electron density at the Wigner-Seitz cell of the corresponding metals

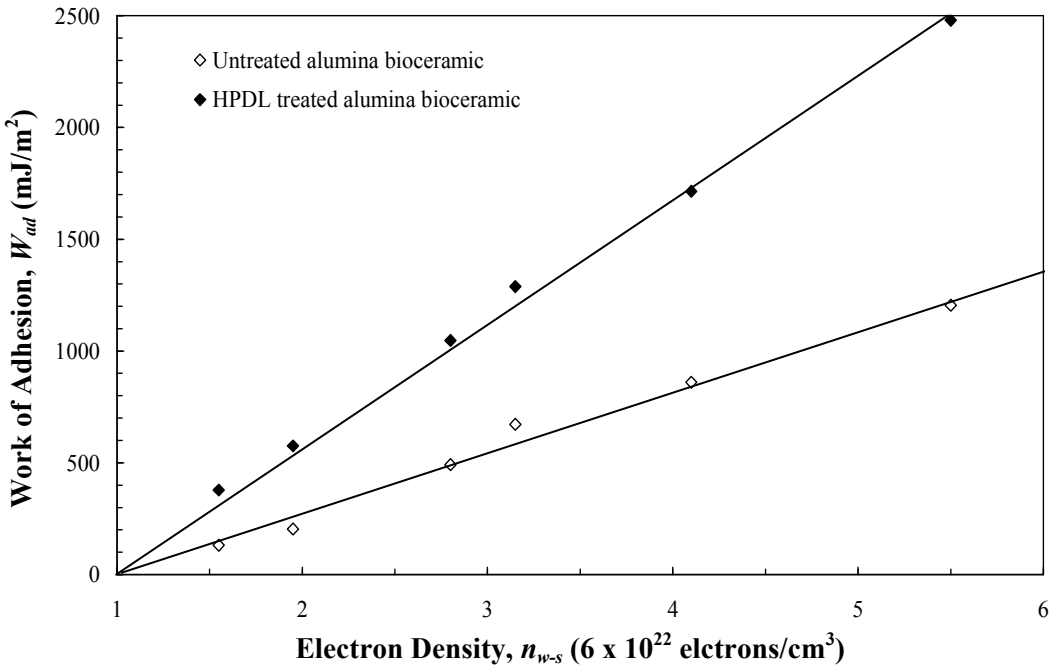

Table 1

Values of typical wettability characteristics for the alumina bioceramic before and after HPDL surface treatment. (40 W laser power, 360 mm/min traverse speed and O_2 process gas)

Property	Alumina Bioceramic Condition	
	Untreated	**HPDL Treated**
Contact Angle, θ		
Human blood	76^0	61^0
Human blood plasma	78^0	63^0
Glycerol	55^0	51^0
4-Octanol	51^0	49^0
Surface Roughness	8.2 μm	5.1 μm
Surface O_2	32.5 at%	44.8 at%
Surface Energy		
Dispersive component, γ_{sv}^{d}	59.2 mJ/m^2	62.0 mJ/m^2
Polar component, γ_{sv}^{p}	0.3 mJ/m^2	1.5 mJ/m^2

Table 2

Experimental mean values of contact angle and calculated values of the work of adhesion for the selected liquid-metals on the untreated and HPDL treated alumina bioceramic. (40 W laser power, 360 mm/min traverse speed and O_2 process gas)

Liquid-Metal	Alumina Bioceramic Condition			
	Untreated		HPDL Treated	
	θ	W_{ad}	θ	W_{ad}
Al	101^0	672 mJ/m^2	61^0	1289 mJ/m^2
Cu	127^0	492 mJ/m^2	100^0	1047 mJ/m^2
Fe	108^0	1205 mJ/m^2	67^0	2480 mJ/m^2
Mn	103^0	860 mJ/m^2	57^0	1715 mJ/m^2
Pb	132^0	131 mJ/m^2	92^0	378 mJ/m^2
Sn	124^0	204 mJ/m^2	78^0	576 mJ/m^2